Utilization of Tannery Sludge in Fly Ash–GGBS Geopolymer: Strength, Microstructure, and Chromium Stabilization

1) Achintya Kumar Mondal, Research Scholar, Civil Engineering Department, Jadavpur University, Jadavpur, Kolkata 700032, India

2) Amit Shiuly, Professor, Civil Engineering Department, Jadavpur University, Jadavpur, Kolkata 700032, India,

Abstract

The accumulation of hazardous industrial waste, specifically tannery sludge (TS), presents a severe environmental challenge due to its toxicity and heavy metal content. This research evaluates the feasibility of valorizing tannery sludge as a partial precursor in fly ash and ground granulated blast furnace slag (GGBS) based geopolymer mortar. The study incorporated sludge at replacement levels ranging from 0% to 25% to analyze its impact on workability, compressive strength, and microstructural evolution. Experimental findings revealed a linear reduction in workability as sludge content increased, primarily driven by the high-water absorption and angular morphology of the waste particles, which raised internal friction. However, mechanical performance demonstrated a distinct optimization pattern. The compressive strength improved significantly up to a 15% replacement level, attaining a peak of 36.0 MPa at 28 days, surpassing the control mix. This enhancement is attributed to the reactive calcium in the sludge, which promotes the formation of supplementary C–A–S–H binding gels that densify the matrix. Conversely, exceeding this 15% threshold resulted in a marked strength decline. This reduction is justified by the "dilution effect," where the scarcity of reactive silica in the sludge interrupts the continuity of the primary N–A–S–H gel network, leading to a weaker structure. Microstructural analysis via SEM corroborated these findings, showing that the optimum mix possessed the most compact matrix with minimal voids. Additionally, X-ray diffraction (XRD) confirmed that hazardous chromium was successfully solidified within the binder as stable Eskolaite.

Keywords: Geopolymer; Tannery sludge; Compressive strength; Microstructure; Waste recycling; Chromium encapsulation.

1. Introduction

The construction industry is increasingly seeking low-carbon binder solutions due to rising environmental concerns [1]. Portland cement (PC), despite its widespread use, remains a major contributor to CO_2 emissions because its production requires high temperatures and significant energy input [2], [3]. In response, alkali-activated binders and geopolymer systems have gained attention as sustainable alternatives. These materials activate aluminosilicate-rich industrial by-products, leading to reduced carbon footprints, enhanced durability, and improved resource efficiency [4], [5], [6].

Fly ash (FA) and ground granulated blast furnace slag (GGBS) are among the most commonly used precursors in geopolymer systems. FA provides reactive silica and alumina that support the formation of a stable three-dimensional aluminosilicate network [7], [8]. GGBS, rich in calcium, accelerates hardening, improves early strength, and forms C–(A)–S–H type gels that complement the N–A–S–H gel structure typically produced by fly ash [9], [10]. Their combined use often results in a hybrid geopolymer matrix with enhanced mechanical and microstructural properties.

In recent years, attention has shifted toward the utilization of challenging industrial wastes, such as tannery sludge, within geopolymer systems. Tannery sludge (TS) is generated in large quantities from leather-processing operations and contains significant amounts of CaO, SiO_2, Al_2O_3, Fe_2O_3, and chromium compounds [11], [12]. Improper management of this waste leads to soil contamination, groundwater pollution, and long-term environmental risks [13]. Researchers have reported that alkali-activated matrices can effectively stabilize heavy metals in tannery sludge and reduce their leachability through chemical binding and physical encapsulation [14], [15]. This makes geopolymer technology a potential solution for both waste utilization and environmental remediation.

Incorporating TS with FA and GGBS can further diversify the chemistry of the binder system. The reactive components in TS may influence gel formation, densification, and strength development, while the alkaline environment of geopolymerization promotes heavy-metal immobilization [16], [17]. Such hybrid systems support the circular economy model by converting multiple industrial wastes into construction-grade materials. However, existing research still offers limited insight into the combined effects of these three components on geopolymer performance, including workability, mechanical behaviour, and microstructure.

This study aims to address these gaps by examining the feasibility and performance of geopolymer composites prepared using FA, GGBS, and TS. The work evaluates their chemical interactions, strength characteristics, microstructural features to support the development of sustainable and low-carbon construction materials.

2. Materials and Methods

2.1 Materials

2.1.1 Fly Ash (FA)

Class F fly ash illustrated in Fig. 1a, was sourced from a local thermal power plant and used as the primary aluminosilicate precursor. The chemical composition of the material was analyzed using X-ray fluorescence (XRF) and is detailed in Table 1. The analysis shows a high combined oxide content (SiO_2 + Al_2O_3 + Fe_2O_3) of 90.31%, which fully meets the standards for Class F fly ash as outlined in ASTM C618 [18]. Before use, the ash was oven-dried at 105 °C to remove any moisture and sieved through a 75 µm mesh to ensure uniform fineness.

2.1.2 Ground Granulated Blast Furnace Slag (GGBS)

Ground Granulated Blast Furnace Slag (GGBS), shown in Fig. 1b, was selected as a calcium-rich co-binder to enhance early-age strength and densify the microstructural network. The slag was obtained from a steel manufacturing plant and ground to a Blaine fineness of 432 m^2/kg. Its chemical composition is presented in Table 1. To assess its reactivity, the Hydraulic Modulus (HM) was calculated using the following equation: $HM = \left\{\frac{CaO+MgO+Al_2O_3}{Sio_2}\right\}$.

The resulting HM value of 1.60 indicates a high latent hydraulic potential, which is suitable for promoting the formation of C–A–S–H gels.

2.1.3 Tannery Sludge (TS)

Dried tannery sludge (TS), displayed in Fig. 1c, was collected from a chrome-tanning facility, dried at 110 °C, pulverized, and sieved to pass through a 90 µm sieve. As shown in Table 1, the sludge contains a significant amount of calcium (14.53%) and heavy metals, particularly Chromium (1.87%). Although its silica content is low (5.37%), the presence of reactive oxides allows it to participate in the alkali-activation process. Consequently, TS was used as a partial precursor replacement to evaluate the binder's ability to immobilize hazardous elements.

Fig. 1. Precursor materials: (a) Fly ash; (b) GGBS; (c) Tannery sludge.

2.1.4 Alkaline Activators

The alkaline activator consisted of a mixture of sodium hydroxide (NaOH) and sodium silicate (Na_2SiO_3) solutions. Commercial-grade NaOH pellets (98% purity) were dissolved to prepare 12 M solutions. These were mixed with sodium silicate (SiO_2/Na_2O) ratio of 2.0. The activator solutions were prepared 24 hours prior to use to ensure thermal stabilization.

2.1.5 Fine Aggregates

Locally available river sand, conforming to Zone II of IS 383[19], was used as fine aggregate. The sand was used in a saturated-surface-dry (SSD) condition to maintain a constant water-to-binder ratio during mixing.

Table.1 Chemical compositions of Fly Ash (FA), GGBS and tannery sludge (TS)

Composition	Fly Ash (%)	GGBS (%)	TS (%)
SiO_2	56.67	39.58	5.37
Al_2O_3	28.16	22.29	7.21
Fe_2O_3	5.48	0.43	5.49
K_2O	1.56	1.35	1.43
CaO	0.78	31.43	14.53
MgO	0.81	9.46	1.68
MnO	0.08	0.15	0.19
Na_2O	0.11	0.15	1.69
Cr	-	-	1.87

Pb	0.012	0.011	0.012
TiO_2	1.98	0.65	0.56

2.2 Mix Proportions

Geopolymer mortar mixes were formulated by varying the proportions of FA, GGBS, and TS, while keeping the total binder content constant, as detailed in Table 2. TS was incorporated as a partial replacement for the aluminosilicate precursor at dosage levels of 5%, 10%, 15%, 20%, and 25% by weight. A fixed fine aggregate-to-binder ratio of 4:1 was maintained for all specimens. Based on preliminary workability trials, an alkaline activator-to-binder ratio of 0.48 was adopted to ensure adequate flow. Throughout the study, the ratio of sodium silicate to sodium hydroxide ($Na_2SiO_3/NaOH$) was held constant at 2.0.

Table 2: Mix Proportions for Geopolymer Mortar (per 1 m³)

Mix	Fly Ash (kg)	GGBS (kg)	TS (kg)	Binder (kg)	Sand (kg)	Sodium Silicate (kg)	Sodium Hydroxide Solution (kg)	Activator Total (kg)
FGS-0	280	120	0	400	1600	133.33	66.67	200
FGS-5	260	120	20	400	1600	133.33	66.67	200
FGS-10	240	120	40	400	1600	133.33	66.67	200
FGS-15	220	120	60	400	1600	133.33	66.67	200
FGS-20	200	120	80	400	1600	133.33	66.67	200
FGS-25	180	120	100	400	1600	133.33	66.67	200

2.3 Mixing and Casting Procedure

The preparation of the geopolymer mortar commenced with the dry mixing of all solid precursors—FA, GGBS, TS and fine aggregates in a mechanical pan mixer for 3 minutes to ensure homogeneity. Subsequently, the pre-mixed alkaline activator solution was introduced gradually to the dry mixture. Mixing continued for an additional 4–5 minutes until a uniform, cohesive mortar paste was achieved. The fresh mortar was then cast into standard cubic moulds (50×50×50 mm), as shown in Fig. 2a, for compressive strength testing. To ensure proper consolidation and remove entrapped air, the mortar was placed in two layers and compacted using a vibration table. Immediately after casting, the moulds were sealed with a polymeric film to prevent moisture loss and left undisturbed at room temperature for 24 hours.

2.4 Curing Regime

Following the initial 24-hour ambient setting period, the specimens were demoulded. Subsequently, the samples were subjected to heat curing in a laboratory oven at 65°C for a duration of 24 hours, as depicted in Fig. 2b, to accelerate geopolymerization kinetics. After this thermal treatment, the specimens were removed from the oven and stored under ambient laboratory conditions (temperature 25–30 °C, relative humidity 60-70%) until the scheduled testing ages of 7and 28days.

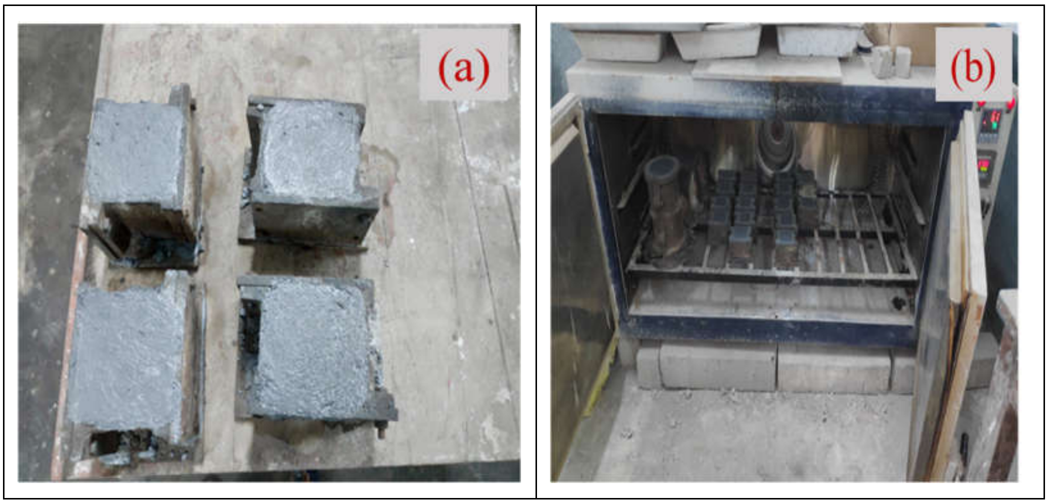

Fig. 2. Specimen preparation: (a) casting of fresh mortar and (b) heat curing at 65°C.

2.5 Testing Methods

2.5.1 Fresh State Properties

The workability of the fresh geopolymer mortar was evaluated using the flow table test in accordance with ASTM C1437 [20]. As illustrated in Fig. 3, the mortar was placed into a standard conical mould in two layers, with each layer tamped 20 times to ensure consolidation (Fig. 3a). After lifting the mould, the flow table was dropped 25 times within 15 seconds. The resulting spread diameter was measured in four directions (Fig. 3b), and the average value was recorded as the flow percentage, providing an index of the mix's consistency and ease of placement.

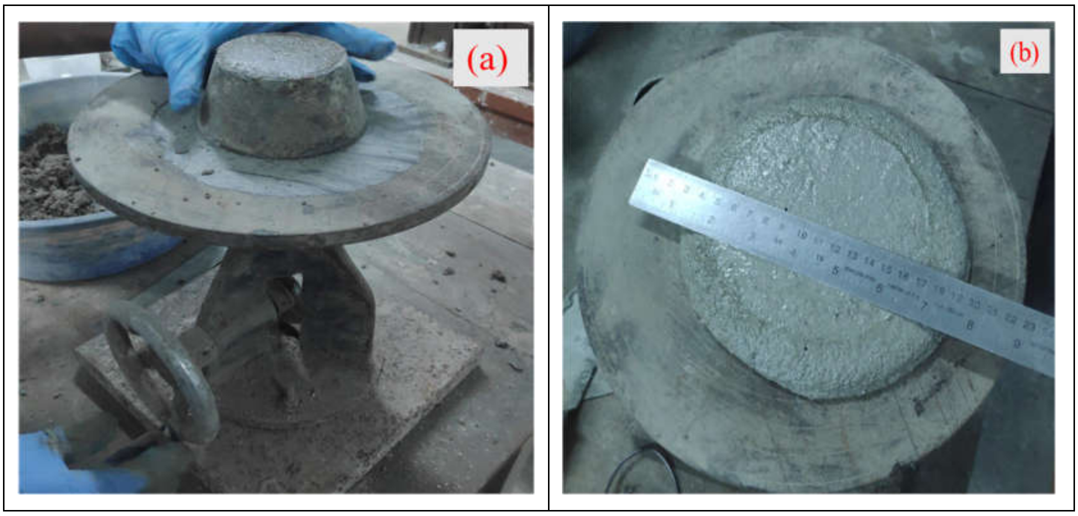

Fig. 3. Flow table test procedure: (a) fresh mortar filled in the standard conical mould; (b) measurement of spread diameter after testing.

2.5.2 Mechanical Strengths

Compressive strength testing was conducted on 50 mm cubic specimens following the guidelines of ASTM C109 [21]. The experimental setup is depicted in Fig. 4. The tests were performed using a universal testing machine (UTM) at a constant loading rate of 0.9 kN/s until failure. Three replicate specimens were tested for each mix at curing ages of 7 and 28 days. The average value was reported as the compressive strength.

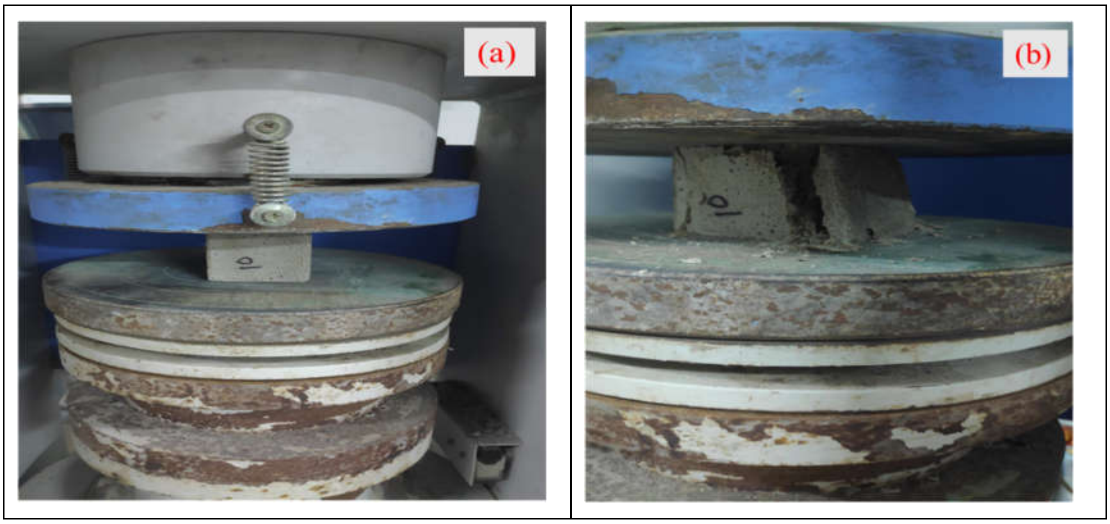

Fig. 4. Compressive strength testing: (a) specimen placement in the loading frame; (b) typical failure mode of the geopolymer mortar cube after testing.

2.5.2 Microstructural Analysis

To investigate the reaction mechanisms and phase changes within the binder matrix, microstructural characterization was performed on selected 28-day cured samples.

- **Scanning Electron Microscopy (SEM):** Fractured surfaces of the specimens were gold-coated and examined using SEM to observe the morphological features, pore structure, and matrix densification. This analysis provided visual evidence of the degree of geopolymerization and the physical encapsulation of waste particles.
- **X-Ray Diffraction (XRD):** Powder X-ray diffraction analysis was conducted to identify the crystalline phases and amorphous gel products formed during the activation process. The diffraction patterns were recorded over a 2θ range of 10° to 80° to detect the presence of geopolymeric gels (N–A–S–H / C–A–S–H) and any unreacted precursor phases.

3. Results and Discussion

3.1 Flow diameter

The flow test results presented in Fig. 5 demonstrate a clear reduction in workability as the tannery sludge content increased. The control mix (FGS-0) exhibited the highest fluidity with a flow diameter of 152 mm, but this value steadily declined to 128 mm at the maximum replacement level of 25% (FGS-25). This 15.8% reduction occurs primarily because TS particles are rough and angular, creating significant internal friction compared to the smooth, spherical fly ash particles that typically facilitate flow [16], [22]. The presence of fibrous organic residues in the sludge further contributes to this effect by increasing viscosity and resisting movement [23].

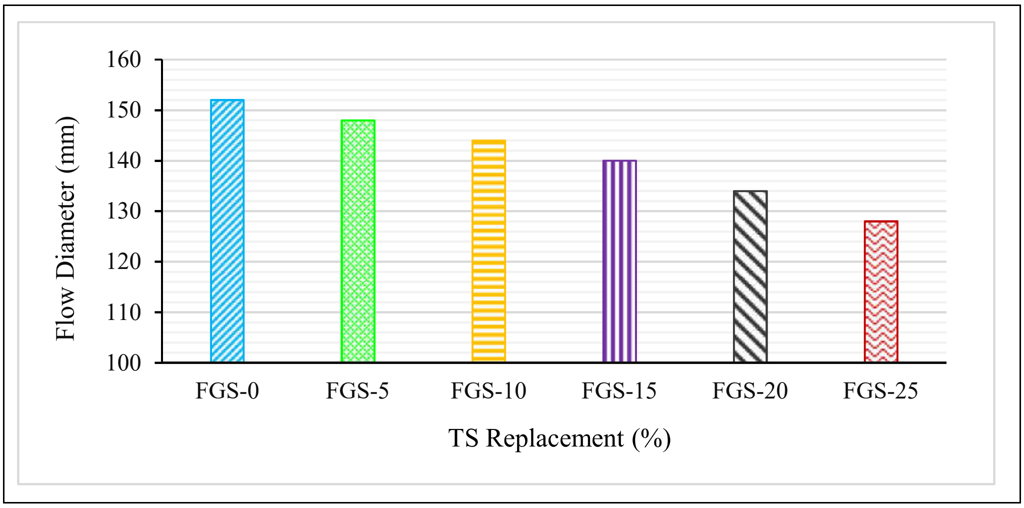

Fig. 5. Variation in flow diameter of geopolymer mortar with increasing tannery sludge replacement.

3.2 Compressive strength

The compressive strength results for 7 and 28 days, illustrated in Fig. 6, indicate that the addition of TS has a noticeable effect on the mortar's performance. At 7 days, the strength increased from 23.5 MPa in the control mix (FGS-0) to a peak of 25.3 MPa at 15% replacement (FGS-15), subsequently decreasing to 21.5 MPa at 25% substitution (FGS-25). A similar trend was observed at 28 days, where the strength rose from 33.5 MPa to a maximum of 36.0 MPa at 15% replacement, followed by a drop to 30.8 MPa. This moderate strength gains up to 15% replacement may be due to the calcium content in the sludge (approx. 14% CaO), which could promote the formation of additional C–A–S–H binding gels that strengthen the matrix [10], [16]. Furthermore, the finer sludge particles might act as a micro-filler, possibly filling small voids to improve density [24]. However, the reduction in strength at higher replacement levels suggests that a "dilution effect" may be occurring. Since tannery sludge contains significantly less silica (5%) than fly ash (56%), replacing a large amount of fly ash could reduce the reactive silica available for binding N–A–S–H gel network [25]. Additionally, the organic residues and heavy metals present in the waste may potentially interfere with the chemical reaction, leading to a weaker structure at higher dosages [26], [27].

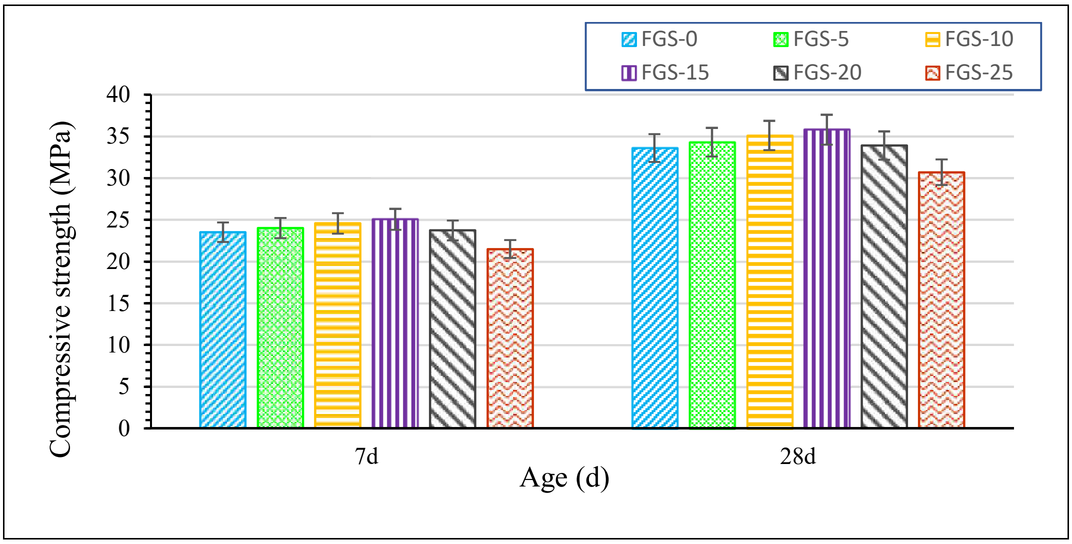

Fig. 6. 7-day and 28-day compressive strength of geopolymer mortar with increasing tannery sludge replacement.

3.3 Microstructure study

3.3.1 SEM

The SEM images in Fig. 7 (a–f) suggest that adding tannery sludge changes the internal structure of the mortar. The control mix (Fig. 7a) appears to have a somewhat porous structure with many loose, partially reacted fly ash particles, which might indicate a weaker bond. However, when sludge was added up to 15% (Fig. 7b–d), the matrix seemed to become denser. The 15% sample (Fig. 7d) looks the most uniform with fewer voids. This improvement could be due to the extra calcium from the sludge, which may help form additional binding gels (C–A–S–H) that fill the gaps and glue the particles together. On the other hand, at higher replacement levels (20–25%), the structure appears to deteriorate. The images for these mixes (Fig. 7e, f) show visible cracks and loose clumps of particles. This breakdown might happen because replacing too much reactive fly ash with sludge could weaken the chemical network. Additionally, the rough and irregular shape of the excess sludge particles may prevent them from packing tightly, which likely contributes to the lower strength and reduced flowability seen in the earlier tests.

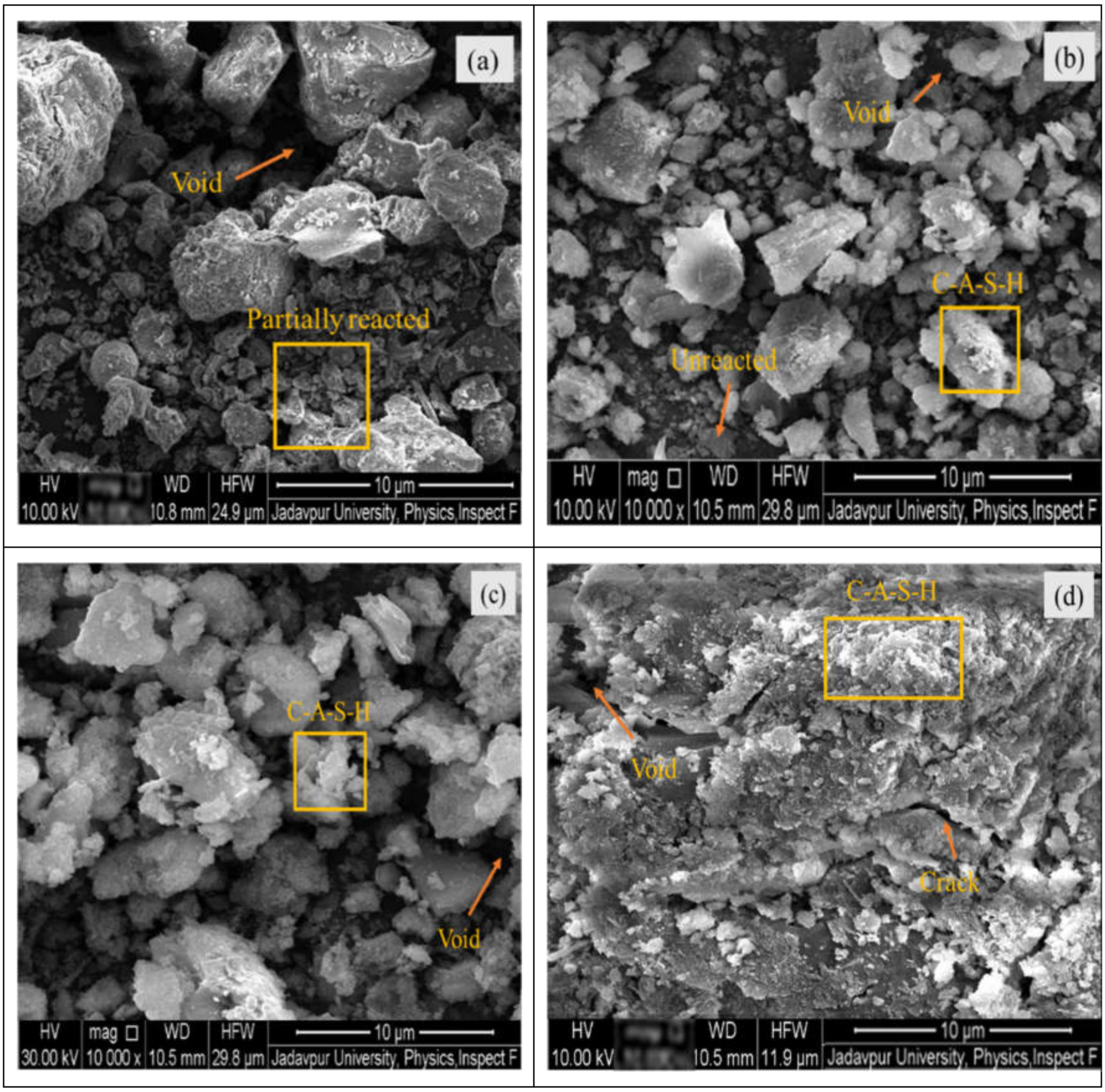

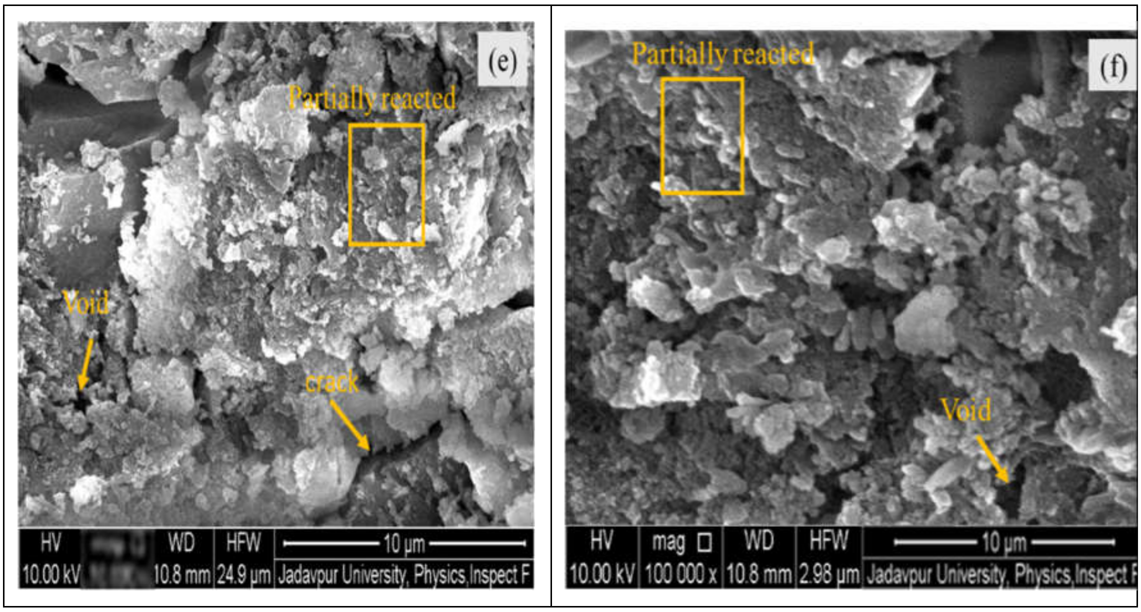

Fig. 7. SEM micrographs of geopolymer mortar with varying tannery sludge content: (a) 0% TS; (b) 5% TS; (c) 10% TS; (d) 15% TS; (e) 20% TS; (f) 25% TS.

3.3.2 XRD

The X-ray diffraction (XRD) patterns, shown in Fig. 8 (a–f), display a broad "hump" between 20° and 35° (2θ), which suggests the formation of the primary N–A–S–H binding gel that holds the mortar together. Alongside this gel, clear crystalline peaks were identified for minerals such as Quartz SiO_2), mullite ($3Al_2O_3$. $2SiO_2$) and calcite ($CaCO_3$) which originate from the unreacted fly ash and tannery sludge. Interestingly, as the sludge replacement increased from 0% to 25%, the intensity of the Quartz and Calcite peaks grew linearly. This trend points to a "filler effect," implying that these inert minerals are mechanically accumulating in the matrix rather than chemically reacting. This mineral build-up contrasts with the strength results; while the mineral peaks kept growing up to 25%, the compressive strength dropped after 15%. This decline suggests that the excessive volume of unreacted minerals may be "diluting" the reactive binder, potentially interrupting the continuity of the amorphous gel network [10], [25]. Additionally, the appearance of a specific peak for Eskolaite (Cr_2O_3) at 42.38° indicates that the trivalent chromium from the sludge is likely being successfully stabilized and encapsulated within the geopolymer structure.

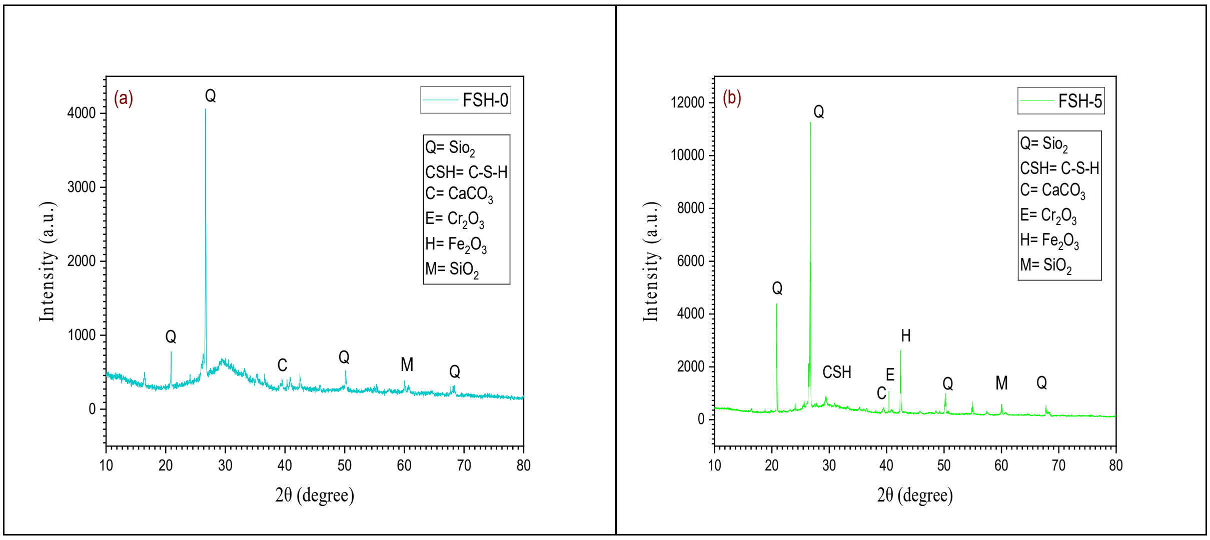

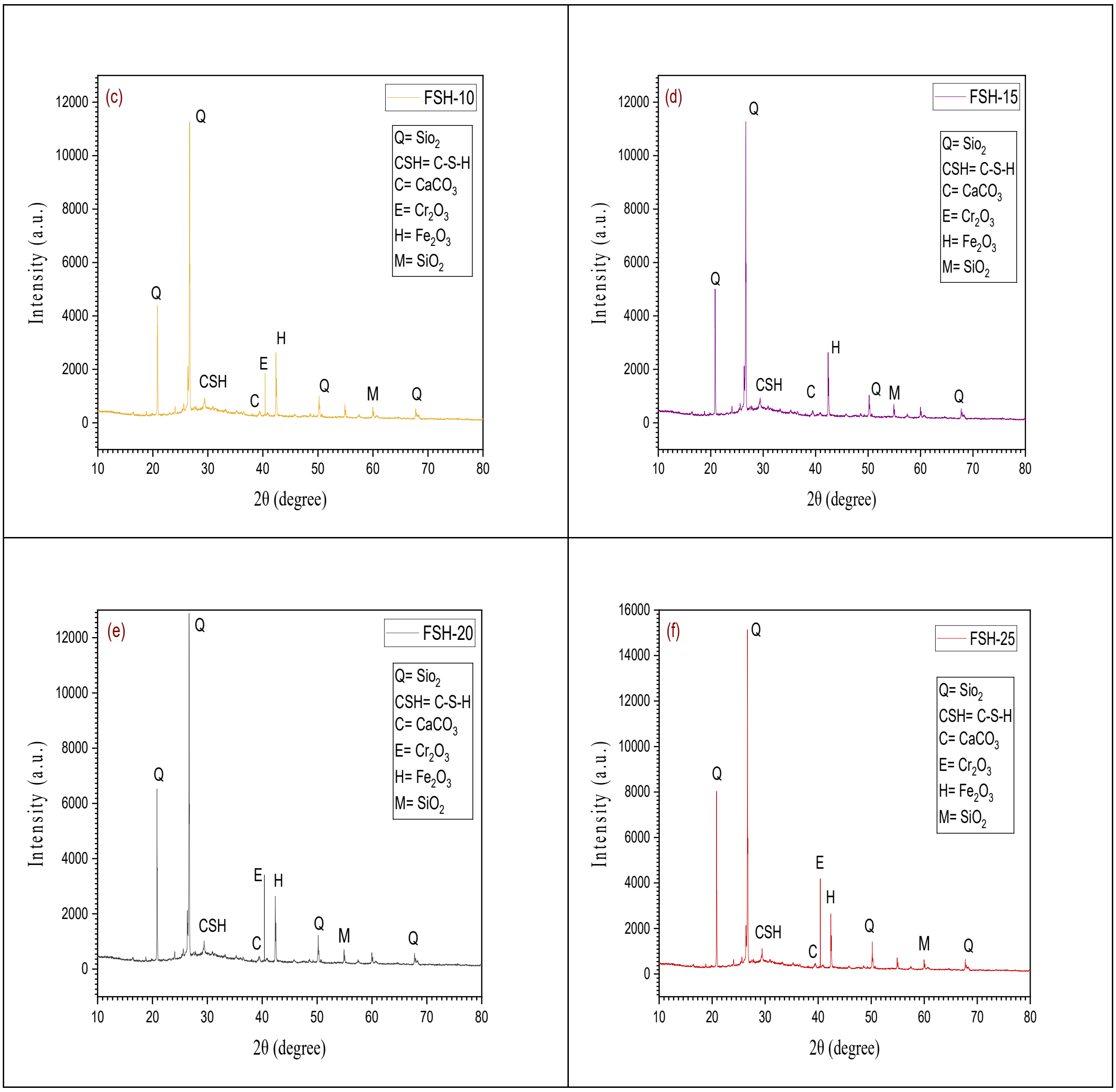

Fig. 8. XRD patterns of geopolymer mortar with increasing tannery sludge content: (a) 0% TS; (b) 5% TS; (c) 10% TS; (d) 15% TS; (e) 20% TS; (f) 25% TS.

4 Conclusion

The experimental results of this study demonstrate that tannery sludge (TS) can be successfully recycled as a partial precursor in fly ash–GGBS geopolymer mortar, provided the replacement level is carefully optimized. The major findings are summarized as follows:

- **Workability Reduction:** The flowability of the fresh mortar decreased linearly as tannery sludge was added, dropping from 152 mm in the control mix to 128 mm at 25% replacement. This reduction occurs because the sludge particles are angular and porous, which increases internal friction and water demand.
- **Optimum Strength at 15%:** The compressive strength improved with moderate sludge addition, reaching a peak of 36.0 MPa at 15% replacement (higher than the 33.5 MPa control). This enhancement is attributed to the calcium in the sludge, which promotes the formation of additional C–A–S–H gels that densify the binder matrix.

- **Strength Loss Mechanism:** Beyond the 15% optimum, strength declined significantly (dropping to 30.8 MPa at 25%). This is caused by the "dilution effect": replacing silica-rich fly ash with silica-poor sludge creates a deficit in the reactive materials needed to build a continuous N–A–S–H gel network, leading to a weaker structure.
- **Microstructure and Safety:** SEM analysis confirmed that the optimum mix exhibited the most compact and uniform microstructure with minimal voids. Furthermore, XRD analysis revealed that the hazardous chromium from the sludge was successfully encapsulated within the geopolymer matrix as the stable mineral Eskolaite (Cr_2O_3).

5 References

[1] "Transforming waste into sustainable building materials: Properties and environmental impacts of Geopolymer concrete with recycled concrete aggregates," *Glob. NEST J.*, Jan. 2024.

[2] C. Shi, B. Qu, and J. L. Provis, "Recent progress in low-carbon binders," *Cem. Concr. Res.*, vol. 122, pp. 227–250, Aug. 2019.

[3] G. A. Ansari and S. S. Kumar, "Geopolymerization of fly ash and GGBS for sustainable industrial waste utilization," *Sci. Rep.*, vol. 15, no. 1, p. 34318, Oct. 2025.

[4] J. L. Provis, "Alkali-activated materials," *Cem. Concr. Res.*, vol. 114, pp. 40–48, Dec. 2018.

[5] B. A. Lanjewar, R. Chippagiri, V. A. Dakwale, and R. V. Ralegaonkar, "Application of Alkali-Activated Sustainable Materials: A Step towards Net Zero Binder," *Energies*, vol. 16, no. 2, p. 969, Jan. 2023.

[6] E. Luga, E. Mustafaraj, M. Corradi, and C. D. Atiş, "Alkali-Activated Binders as Sustainable Alternatives to Portland Cement and Their Resistance to Saline Water," *Materials (Basel).*, vol. 17, no. 17, p. 4408, Sep. 2024.

[7] X. Y. Zhuang *et al.*, "Fly ash-based geopolymer: clean production, properties and applications," *J. Clean. Prod.*, vol. 125, pp. 253–267, Jul. 2016.

[8] T. Krishnan and R. Purushothaman, "Characterization of Fly Ash Sources in the Synthesis of Geopolymer," *Silicon*, vol. 14, no. 6, pp. 2635–2646, Apr. 2022.

[9] P. Nath and P. K. Sarker, "Effect of GGBFS on setting, workability and early strength properties of fly ash geopolymer concrete cured in ambient condition," *Constr. Build. Mater.*, vol. 66, pp. 163–171, Sep. 2014.

[10] C. K. Yip, G. C. Lukey, and J. S. J. van Deventer, "The coexistence of geopolymeric gel and calcium silicate hydrate at the early stage of alkaline activation," *Cem. Concr. Res.*, vol. 35, no. 9, pp. 1688–1697, Sep. 2005.

[11] A. Kowalik-Klimczak *et al.*, "Valorisation of Tannery Waste to Recover Chromium with a View to Reusing It in Industrial Practise," *Membranes (Basel).*, vol. 14, no. 6, p. 136, Jun. 2024.

[12] M. Haroun, A. Idris, and S. Omar, "Characterisation and Composting of Tannery Sludge," 2007.

[13] A. Bhardwaj, S. Kumar, and D. Singh, "Tannery effluent treatment and its environmental impact: a review of current practices and emerging technologies," *Water Qual. Res. J.*, vol. 58, no. 2, pp. 128–152, May 2023.

[14] C. Sgarlata *et al.*, "Sustainable Chromium Encapsulation: Alkali Activation Route," *Front. Mater.*, vol. 9, Jul. 2022.

[15] W. Zhang, S. Li, J. Ma, D. Huang, L. Zhang, and C. Ma, "Feasibility Study of the Synergistic Use of Sludge and Coal-Based Solid Waste to Produce Environmentally Friendly Grouting Materials," *ACS Omega*, vol. 8, no. 48, pp. 45854–45866, Dec. 2023.

[16] S. Chen, P. Duan, M. Zhao, H. Shi, and Y. Bie, “Solidification Mechanism and Strength Characteristics of Alkali-Activated Tannery Sludge–Slag Geopolymer,” *Buildings*, vol. 14, no. 4, p. 1060, Apr. 2024.

[17] M. Jothilingam, V. Preethi, P. Sri Chandana, and G. Janardhanan, “Fabrication of sustainable green bricks by the effective utilization of tannery sludge as main additive,” *Structures*, vol. 48, pp. 182–194, Feb. 2023.

[18] K. Jafari and F. Rajabipour, “Performance of Impure Calcined Clay as a Pozzolan in Concrete,” *Transp. Res. Rec. J. Transp. Res. Board*, vol. 2675, no. 2, pp. 98–107, Feb. 2021.

[19] IS 383 : 2016, “Specification for Coarse and Fine Aggregates From Natural Sources for Concrete,” *Bureau of Indian Standards,New Delhi*. pp. 1–24, 2016.

[20] H. Page, *Design and Control of Concrete Mixtures, EB001*, no. 54048. 1996.

[21] A. C109/109M-16a, “Standard test method for compressive strength of hydraulic cement mortars (Using 2-in. or cube specimens),” *Annu. B. ASTM Stand.*, pp. 1–10, 2016.

[22] P. Chindaprasirt, T. Chareerat, and V. Sirivivatnanon, “Workability and strength of coarse high calcium fly ash geopolymer,” *Cem. Concr. Compos.*, vol. 29, no. 3, pp. 224–229, Mar. 2007.

[23] O. Kizinievic, V. Kizinievic, and J. Malaiskiene, “Use of Tannery Sludge in Clay Brick Manufacturing,” *Environ. Eng. Manag. J.*, vol. 19, no. 5, pp. 839–848, 2020.

[24] A. Hanani Ismail, A. Kusbiantoro, Y. Tajunnisa, J. Jaya Ekaputri, and I. Laory, “A review of aluminosilicate sources from inorganic waste for geopolymer production: Sustainable approach for hydrocarbon waste disposal,” *Clean. Mater.*, vol. 13, p. 100259, Sep. 2024.

[25] P. Duxson, J. L. Provis, G. C. Lukey, and J. S. J. van Deventer, “The role of inorganic polymer technology in the development of ‘green concrete,’” *Cem. Concr. Res.*, vol. 37, no. 12, pp. 1590–1597, Dec. 2007.

[26] J. Chen, J. Zhou, S. Chen, H. Shi, Q. Hu, and Y. Tang, “Evaluation of slag and tannery sludge based geopolymer after thermal exposure: Properties, phase transformation and Cr leaching behavior,” *J. Clean. Prod.*, vol. 512, p. 145716, Jun. 2025.

[27] M. A. I. Juel, A. Mizan, and T. Ahmed, “Sustainable use of tannery sludge in brick manufacturing in Bangladesh,” *Waste Manag.*, vol. 60, pp. 259–269, Feb. 2017.